SUPPRTING INFORMATION

Optimization of SnO_2-Based Electron Transport Layer Using Cerium Oxide for Efficient and Stable Perovskite Solar Cells

Zhipeng Liu[1], Zhiwei Gu[1], Yang Lv[1], Zhiqin Su[1], Jian Sun[1], Linlin Qiu[3,]*, Pingfan Du[1, 2,]*

[1] *College of Textile Science and Engineering, Zhejiang Sci-Tech University, Hangzhou 310018, PR China*

[2] *Key Laboratory of Intelligent Textile and Flexible Interconnection of Zhejiang Province, Zhejiang Sci-Tech University, Hangzhou 310018, PR China*

[3] *College of Textile and Apparel, Quanzhou Normal University, Quanzhou 362000, China*

*Corresponding author. Tel.: fax: +86 571 86843603

E-mail addresses: dupf@zstu.edu.cn (P. Du); qiull@qztc.edu.cn (L. Qiu)

Experimental Section

Materials: Cerium (III) acetylacetonate hydrate and ethanol were provided by Shanghai Macklin Biochemical Co., Ltd. The ITO glass substrates were fabricated by Advanced Election Technology Co., Ltd. Lead (II) iodide (PbI_2, 99.99%), formamidinium iodide (FAI, 99.5%), methylammonium bromide (MABr, 99.5%), cesium iodide (CsI, 99.99%), Tris[4-(1, 1-dimethylethyl)-2-(1H-pyrazol-1-yl)pyridine]cobaltsaltwith1, 1, 1-trifluoro-N-[(trifluoromethyl)sulfonyl]methanesulfonamide (FK209 Co(III) TFSI, 98%), lithium bis(trifluoromethanesulfonyl)imide (Li-TFSI, 99.95%), 4-tert-butylpyridine (t-BP, 96%), 2, 2′, 7, 7′-Tetrakis(*N*, *N*-di-*p*-methoxyphenylamine)-9, 9′-spirobifluorene (spiro-OMeTAD, 99.5%) and phenyl-C61-butyric acid methyl ester ($PC_{61}BM$, 99%) were purchased from Xi'an Polymer Light Technology Corp. SnO_2 colloidal solution (15% in water) was purchased from Alfa Aesar. Dimethyl formamide (DMF, 99.8%, anhydrous), dimethyl sulfoxide (DMSO, 99.9%, anhydrous), isopropanol (IPA, 99.7%), chlorobenzene (CB, 99.8%, anhydrous), and acetonitrile (ACN, 99.8%, anhydrous) was supplied by Aladdin. All chemicals were used as received without further purification.

SnO_2/CeO_x ETLs fabrication: the colloidal SnO_2 aqueous dispersion solution was diluted using deionized water to 2.14 wt% to obtain SnO_2 precursor. Then Cerium (III) acetylacetone hydrate was added to ethanol at a solution concentration of 2 mg/ml and then treated in an ultrasonic bath for 30 min to obtain a CeO_x precursor solution. These precursors were then spin-coated onto pre-cleaned ITO glasses at a rate of 4000 rpm for 30s, followed by thermal annealing at 150 ℃ for 30 min in ambient air, to fabricate SnO_2

and SnO_2/ CeO_x ETLs.

Perovskite precursor solution: The perovskite precursor was prepared with PbI_2 (742.2 mg), FAI (224.4 mg), MABr (16.2 mg), and CsI (19.8 mg) are dissolved into anhydrous DMF/DMSO (v/v: 8:2) mixed solution and stirred at room temperature for 5 h.

Device fabrication: Firstly, the (indium tin oxide) ITO glass substrates were sequentially cleaned with detergent adding into deionized water, acetone, and ethanol for 15 min each in an ultrasonic bath. The glass substrates were cleaned with IPA at 5000 rpm for 15 s, and then dried at 60 °C for 10 min. Before depositing the ETL films and the perovskite films, all the substrates were further treated with UV-ozone for 15 min. The perovskite films were deposited onto the ETL substrates via a two-step spin-coating at 1000 r/10 s and 5000 r/30 s. After the perovskite precursor were dropped, the antisolvent EA were rapidly dropped on the center of substrate 15 s prior to the end of the program, the as-prepared perovskite films were annealed at 150 °C for 30 min. Upon cooling to room temperature, The HTL precursor solution was prepared by mixing 70 mg of Spiro-OMeTAD power, 20 μL of t-BP, and 70 μL of Li-TFSI solution (170 mg Li-TSFI dissolve in 1 mL ACN) and 50 μL of FK209 Co (III) TFSI Salt (150 mg/mL in ACN) in 1 mL of CB, was spin-coated on the top of the perovskite films at 4000 rpm for 30 s. Finally, an Ag electrode with a thickness of 80 nm with an active area of 0.06 cm^2 was deposited by thermal evaporation. All devices were assembled in ambient air with a relative humidity of 25-35% and a temperature of 18-23 °C.

Characterization: Top-view and cross-sectional scanning electron microscopy (SEM)

images were characterized through a Field-emission scanning electron microscope (FE-SEM, Ultra 55, Zeiss, Germany) with an electron beam accelerated voltage at 3 kV. The CeO_x nanoparticles were observed by transmission electron microscopy (TEM, JEOLJEM 2100) at 200 kV. Wide-angle XRD measurements were implemented with a Bruker D8 Advance instrument using a Cu Kα source (40 kV, 1.54 Å) with an incidence angle of 1.0°. X-ray photoelectron spectroscopy (XPS, K-Alpha, USA) is performed using a micro-focus monochromatic Al Kα X-ray source, corresponded to the instrument resolution of 0.45 eV. UPS was carried out by using an ultraviolet photoelectron spectrometer (ESCALAB 250Xi, Thermo Fisher). The UV-visible absorption and transmission spectra were recorded by a UV-Visible spectrophotometer (UV-vis, P4, China). The electrochemical impedance spectroscopy (EIS) is measured by a potentiostat (Im6ex/Zahner) to explore charge transfer properties and battery performance with an alternative signal amplitude of 10 mV and a frequency range of 0.01-100 kHz. The steady-state photoluminescence (PL) spectrum PL and Time-resolved PL (TRPL) decay were measured via Fluo Time 300 fluorophotometer Lifetime Spectrometer. Incident photo-to-current conversion efficiency (IPCE) curves are recorded using a quantum efficiency (QE)/IPCE measured system (Solar Cell Scan 100/Zolix) and calibrated by a monocrystalline silicon diode. The *J–V* characteristics of PSCs were measured with a source meter (2400-SCS, Keithley) under AM1.5 radiation (1 sun conditions, 100 mW cm^{-2}).

Equation S1. Gaussian function for peak analysis and peak fitting:

$$y = y_0 + \frac{Ae^{\frac{-4In(2)(x-x_c)^2}{w^2}}}{w\sqrt{\frac{\pi}{4In(2)}}} \quad \textbf{(S1)}$$

y_0 represents the ordinate position of the baseline, A is constant, x_c is the abscissa corresponding to the highest intensity of the diffraction peak, and w represents the half-peak width value (FWHM).

Equation S2. The Debye-Scherrer formula:

$$D = \frac{k\lambda}{w\cos\theta} \quad \textbf{(S2)}$$

D represents the grain size, k is constant, λ is the incidence wavelength of X-rays, θ is the diffraction angle, and w represents the FWHM value.

Equation S4. The PL decay curves were fitted using the following bi-exponential decay function:

$$Y = A_1\exp\left(-\frac{t}{\tau_1}\right) + A_2\exp\left(-\frac{t}{\tau_2}\right) + y_0, \quad \textbf{(S3)}$$

where A_1 and A_2 are constants representing the contributions of the fast and slow components, respectively. The fast transient component, τ_1, is linked to the surface characteristics, while the slow transient component, τ_2, is linked to the volume characteristics. y_0 is an offset constant.

Equation S5. The average TRPL lifetime was calculated according to:

$$\tau_{ave} = \frac{A_1 * \tau_1^2 + A_2 * \tau_2^2}{A_1 * \tau_1 + A_2 * \tau_2}. \quad \textbf{(S4)}$$

Equation S6. The open-circuit voltage dependence on light intensity was fitted using

the following equation:

$$V_{oc} = \frac{nkT}{q} ln(I) \quad \textbf{(S5)}$$

where n is the ideality factor, k is the Boltzmann constant, T is the absolute temperature, q is the elementary charge, and I is the light intensity.

Equation S7. The trap density was calculated using the following equation:

$$N_{defects} = \frac{2\varepsilon_0 \varepsilon V_{TFL}}{eL^2} \quad \textbf{(S6)}$$

where ε_0 is the vacuum permittivity, ε is the relative dielectric constant of the perovskite, e is the electron charge, and L is the thickness of the perovskite layer.

Equation S8. The hysteresis index of the PSCs was calculated according to the following equation:

$$Hysteresis\ index = \frac{PCE_{Reverse} - PCE_{Forward}}{PCE_{Reverse}} \times 100\% \quad \textbf{(S7)}$$

Figure S1. Optical image of CeO_x precursor solution.

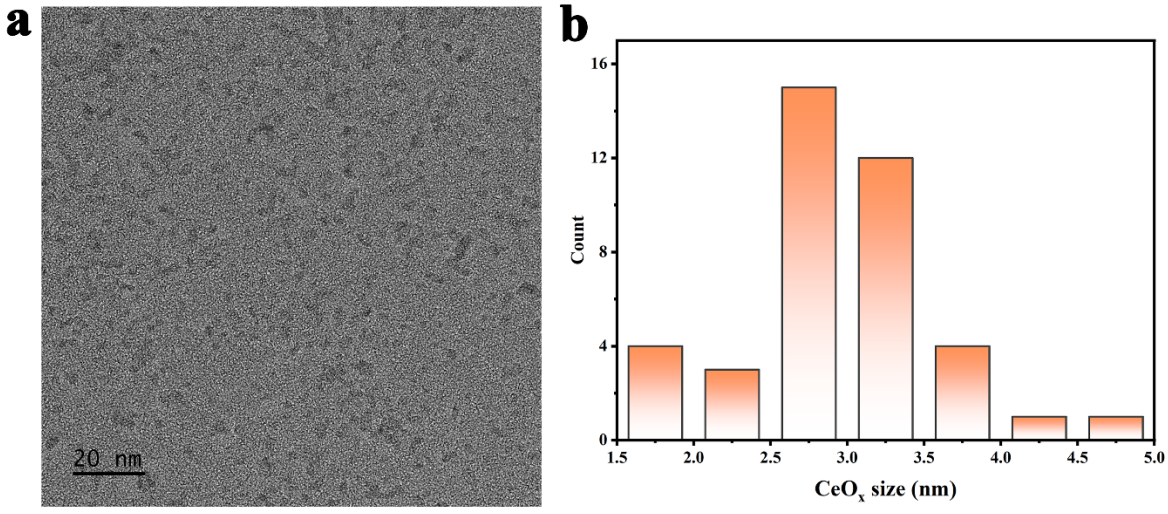

Figure S2. (a) TEM image and (b) size distribution of CeOx.

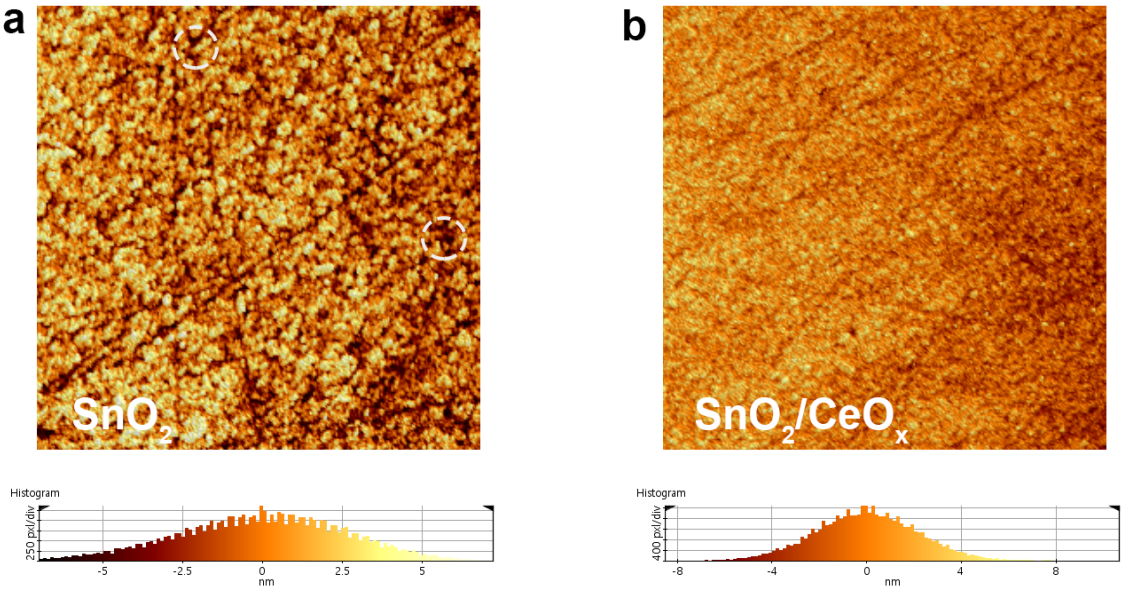

Figure S3. The top view AFM images and normal distribution chart of (a) SnO_2 and (b) SnO_2/CeO_x films.

Figure S4. Optical image of the pristine SnO_2 and SnO_2/CeO_x films deposited on the glass/ITO substrate.

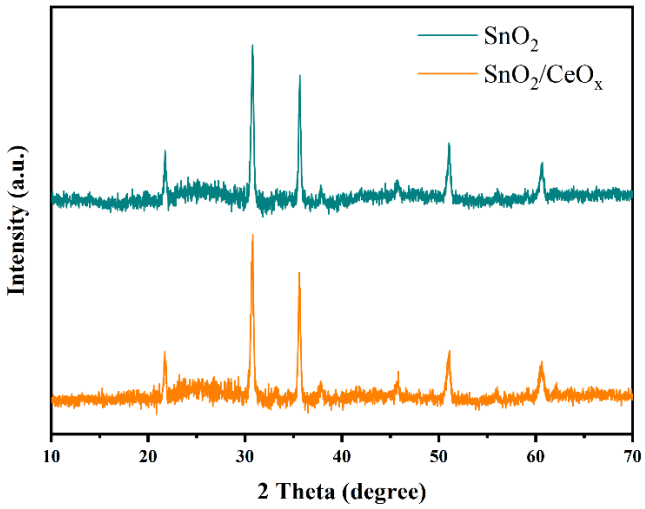

Figure S5. XRD patterns of SnO_2 and SnO_2/ CeO_x films.

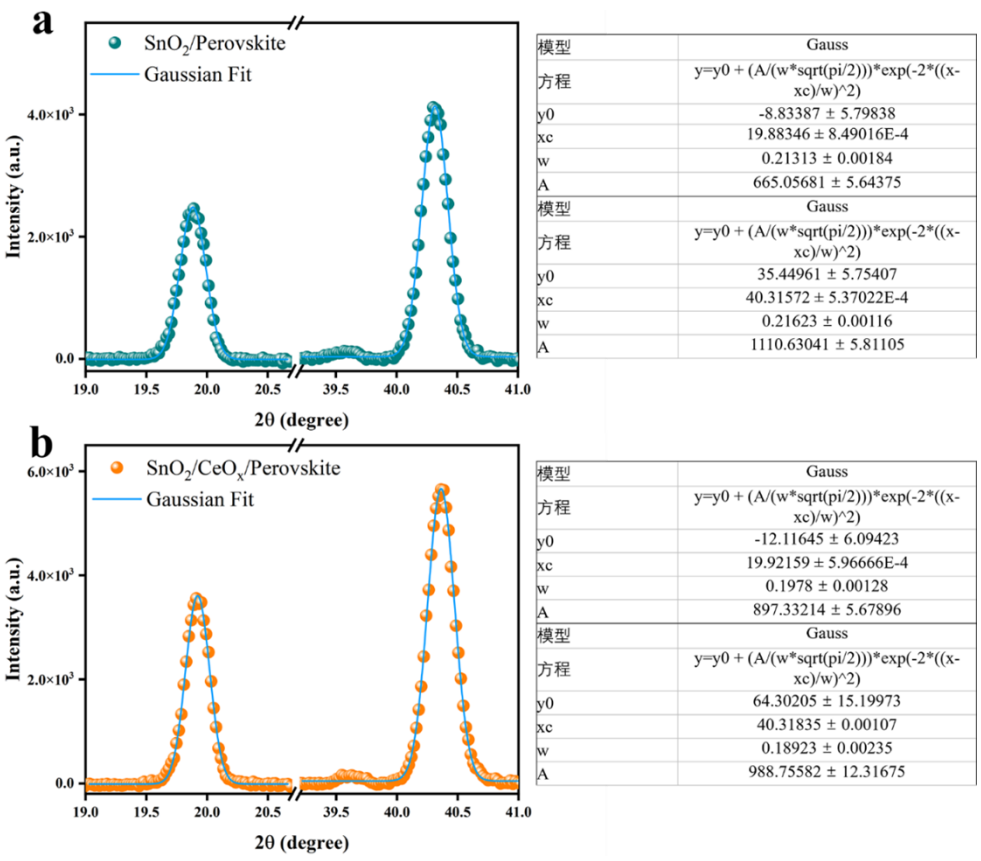

模型	Gauss
方程	y=y0 + (A/(w*sqrt(pi/2)))*exp(-2*((x-xc)/w)^2)
y0	-8.83387 ± 5.79838
xc	19.88346 ± 8.49016E-4
w	0.21313 ± 0.00184
A	665.05681 ± 5.64375

模型	Gauss
方程	y=y0 + (A/(w*sqrt(pi/2)))*exp(-2*((x-xc)/w)^2)
y0	35.44961 ± 5.75407
xc	40.31572 ± 5.37022E-4
w	0.21623 ± 0.00116
A	1110.63041 ± 5.81105

模型	Gauss
方程	y=y0 + (A/(w*sqrt(pi/2)))*exp(-2*((x-xc)/w)^2)
y0	-12.11645 ± 6.09423
xc	19.92159 ± 5.96666E-4
w	0.1978 ± 0.00128
A	897.33214 ± 5.67896

模型	Gauss
方程	y=y0 + (A/(w*sqrt(pi/2)))*exp(-2*((x-xc)/w)^2)
y0	64.30205 ± 15.19973
xc	40.31835 ± 0.00107
w	0.18923 ± 0.00235
A	988.75582 ± 12.31675

Figure S6. (a) The Gaussian fitting results of the perovskite film based on SnO_2; (b) The Gaussian fitting results of the perovskite film based on SnO_2/CeO_x.

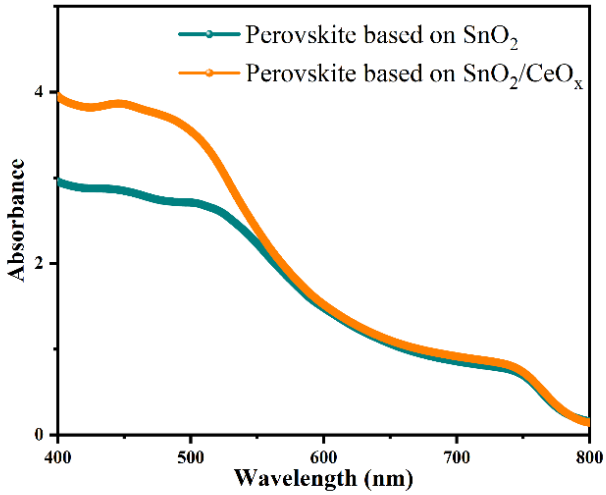

Figure S7. UV–Vis absorbance spectra for perovskite layers deposited on the SnO_2 and SnO_2/CeO_x films.

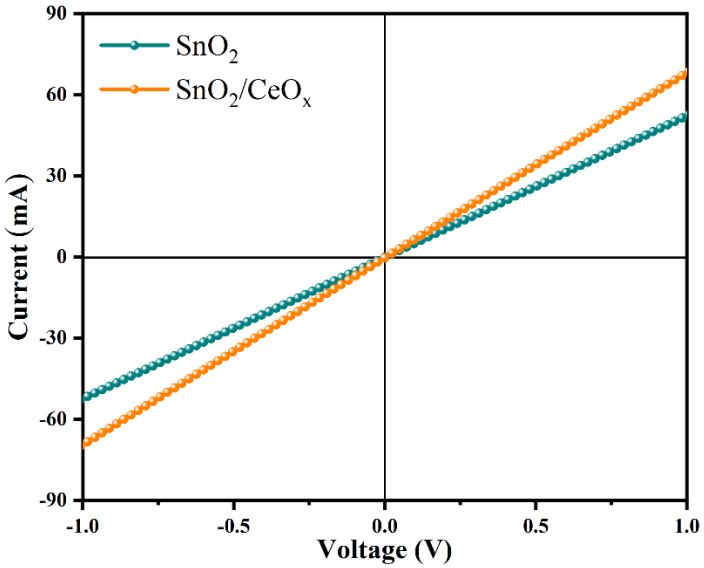

Figure S8. Dark *J–V* curves of the ITO/ETL/Ag structure.

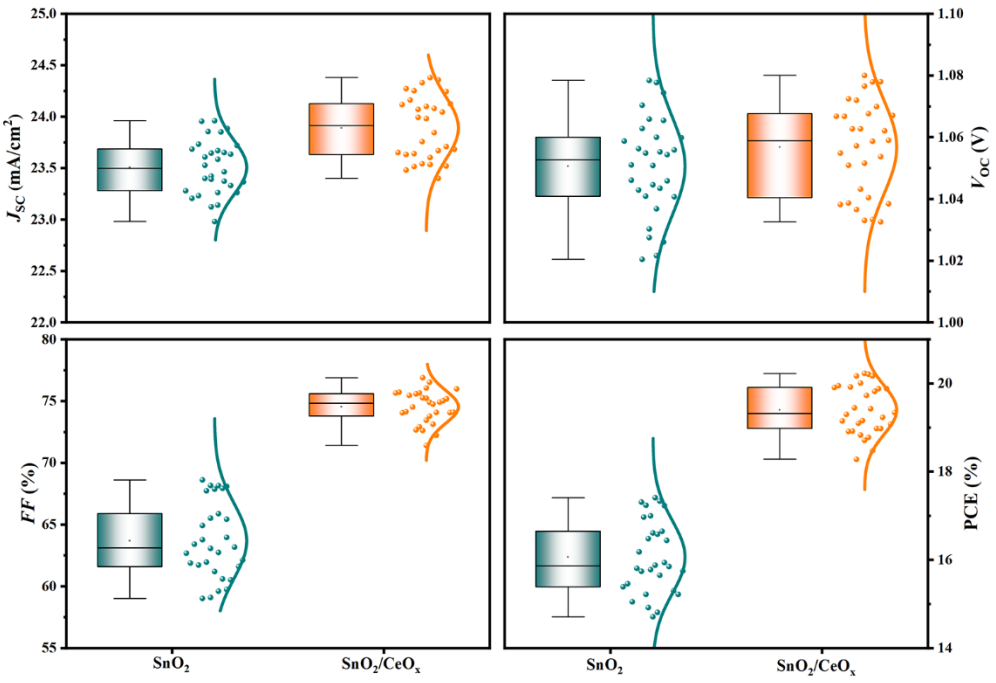

Figure S9. Box plots of the J_{SC}, V_{OC}, *FF*, and *PCE* of PSC devices based on the SnO_2 and SnO_2/CeO_x ETLs.

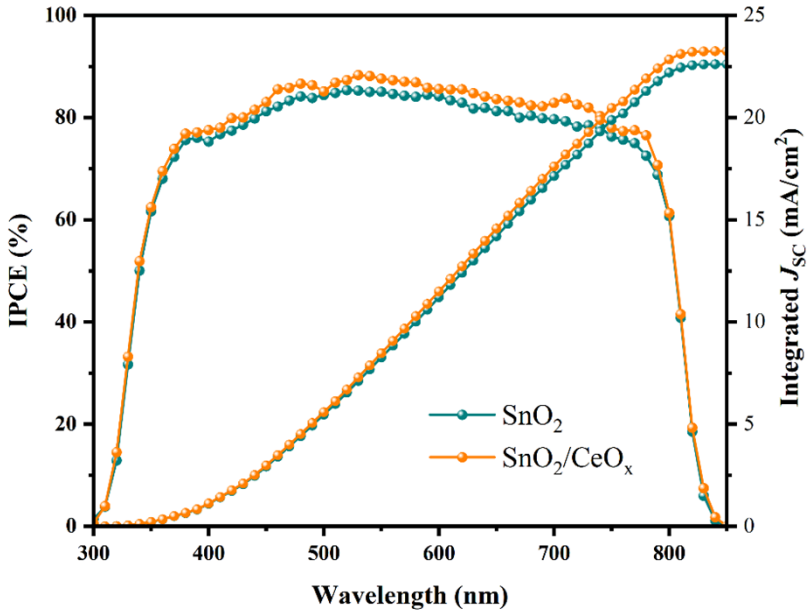

Figure S10. IPCE spectra and integrated J_{SC} values of the devices with CeO_x interlayer and the pristine one.

Table S1. The summarization of Ce 3d XPS data of CeO_x.

Ce 3*d*										
u'''	u''	u'	u	u_0	v'''	v''	v'	v	v_0
916.52 eV	907.35 eV	903.94 eV	900.93 eV	898.93 eV	898.21 eV	888.27 eV	885.38 eV	882.08 eV	880.12 eV

Table S2. The stoichiometric ratio of O/Ce from EDS mapping data corresponding to Figure 2d.

Elements	O K	Si K	Ce L	Total amount
Weight percentage	18.19	0.04	81.77	100.00
Atomic percentage	65.87	0.33	33.80	

*All analyzed elements have been normalized.

Table S3. The calculation results of the XRD FWHM of the perovskite layer on SnO_2 with and without CeO_x, corresponding to Figure 3f and S6.

Sample	2θ	y_0	x_c	A	w *(angle)*
SnO_2/perovskite	19.88°	-8.83387	19.88346	665.05681	0.21313
	40.32°	35.44961	40.31572	1110.63041	0.21623
SnO_2/CeO_x/perovskite	19.92°	-12.11645	19.92159	897.33214	0.19780
	40.32°	64.30205	40.31835	988.75582	0.18923

Table S4. Calculated UPS parameters for SnO_2 and CeO_x films.

ETLs	$E_{cut\text{-}off}$ (eV)	E_{onset} (eV)	E_F (eV)	*VBM* (eV)	E_g (eV)	*CBM* (eV)
SnO_2	16.55	3.70	4.67	8.37	4.02	4.35
CeO_x	17.02	3.40	4.20	7.60	3.50	4.10

Table S5. Fitting parameters of the TRPL curves.

Sample	A_1	τ_1 (ns)	A_2	τ_2 (ns)	τ_{ave} (ns)
SnO_2	0.17571	46.76	0.74740	123.15	116.89
SnO_2/CeO_x	0.77539	2.66	0.75845	57.41	54.93

Table S6. Fitting parameters (R_s and R_{rec}) of PSCs based on different ETLs derived from Figure 5c.

Sample	R_s (Ω)	R_{rec} (Ω)
SnO_2	28.5	21305.2
SnO_2/CeO_x	21.4	22954.4

Table S7. The full photovoltaic parameters for fabricated PSCs corresponding to Figure 6a.

Device	J_{SC} (mA cm^{-2})	V_{OC} (V)	*FF* (%)	*PCE* (%)
SnO_2	23.47 ± 0.49	1.05 ± 0.03	63.82 ± 4.80	16.06 ± 1.35
SnO_2/CeO_x	23.89 ± 0.49	1.06 ± 0.03	74.16 ± 2.76	19.26 ± 0.98

Table S8. Mean values and standard deviation (δ) for 30 devices with SnO_2 ETL and SnO_2/CeO_x ETL.

Device		J_{SC} (mA cm^{-2})	V_{OC} (V)	*FF* (%)	*PCE* (%)
SnO_2	Average	23.51	1.05	63.68	16.06
	δ	± 0.26	± 0.016	± 3.04	± 0.83
SnO_2/CeO_x	Average	23.89	1.06	74.54	19.40
	δ	± 0.31	± 0.015	± 1.33	± 0.56

Table S9. Photovoltaic parameters of the control devices and the best devices under reverse (1.2 V → −0.1 V) and forward (−0.1 V → 1.2 V) scans.

Device		J_{SC} (mA cm^{-2})	V_{OC} (V)	*FF* (%)	*PCE* (%)	*HI* (%)
SnO_2	Reverse	23.95	1.06	68.6	17.41	13.09
	Forward	23.78	1.04	61.2	15.13	
SnO_2/CeO_x	Reverse	24.35	1.08	76.9	20.23	3.01
	Forward	24.28	1.08	74.8	19.62	